Journal of Power Sources 193 (2009) 656–664

Contents lists available at ScienceDirect

Journal of Power Sources

journal homepage: www.elsevier.com/locate/jpowsour

Model of a novel pressurized solid oxide fuel cell gas turbine hybrid engine

Winston Burbank Jr.[a,*], Dr. Dennis Witmer[a], Frank Holcomb[b,1]

[a] Alaska Center for Energy and Power, University of Alaska Fairbanks, Fairbanks, AK, USA
[b] US Army Engineer Research & Development Center, Construction Engineering, Research Laboratory, Champaign, IL, USA

ARTICLE INFO

Article history:
Received 3 February 2009
Received in revised form 4 April 2009
Accepted 9 April 2009
Available online 18 April 2009

Keywords:
SOFC
Solid oxide fuel cell
Gas turbine
Hybrid
Engine
High efficiency
Turndown
Off-design
Model
Steady-state

ABSTRACT

Solid oxide fuel cell gas turbine (SOFC-GT) hybrid systems for producing electricity have received much attention due to high-predicted efficiencies, low pollution and availability of natural gas. Due to the higher value of peak power, a system able to meet fluctuating power demands while retaining high efficiencies is strongly preferable to base load operation. SOFC systems and hybrid variants designed to date have had narrow operating ranges due largely to the necessity of heat management within the fuel cell. Such systems have a single degree of freedom controlled and limited by the fuel cell. This study will introduce a new SOFC-GT hybrid configuration designed to operate over a 5:1 turndown ratio, while maintaining the SOFC stack exit temperature at a constant 1000 °C. The proposed system introduces two new degrees of freedom through the use of a variable-geometry nozzle turbine to directly influence system airflow, and an auxiliary combustor to control the thermal and power needs of the turbomachinery.

1. Background and introduction

Fuel cells are devices that convert the chemical energy of a fuel into electrical energy through an electrochemical reaction, and will operate as long as fuel and oxygen are supplied. While this mechanism avoids some of the losses of heat engines, not all of the energy of the fuel is converted to electricity, and some heat is produced (up to half the energy of the fuel). In high temperature fuel cell systems (such as molten carbonate and solid oxide fuel cells (SOFC)), heat is removed through the exiting gas stream, and temperatures are managed by adjusting the inlet air flow, often to levels several times that required for a stoichiometric reaction [1]. This necessity of excess air for heat removal, supplied by a fan or compressor, has a significant parasitic effect on a fuel cell system, reducing its overall efficiency.

The need to supply high rates of airflow and remove heat suggests a natural mating of high temperature fuel cells and gas turbines, thus creating a fuel cell gas turbine hybrid. In a solid oxide fuel cell gas turbine (SOFC-GT) hybrid there is a synergistic effect in replacing or supplementing the combustor of a typical gas turbine engine with a high temperature fuel cell. The hybrid system is seen to have several benefits over that of a non-hybrid fuel cell system: higher electrochemical efficiency, lower parasitic losses, and additional electrical energy supplied from the turbine. (It is worth noting that most conventional diesel engines are hybrid systems, with the turbocharger providing excess air at increased pressures, resulting in better temperature management of the combustion process and higher efficiency).

Direct SOFC-GT hybrids are made by the placement of the SOFC within the turbomachinery, replacing the combustor and requiring the fuel cell to operate under pressure. An indirect SOFC-GT hybrid places the SOFC after the turbine and uses a heat exchanger to transfer heat from the SOFC exhaust to the air exiting the final stage of compression, but allows the fuel cell to operate at atmospheric pressures. A heat exchanger may also be incorporated into direct systems for improved efficiency. As the most noticeable difference in configurations is the pressure at which air is supplied to the SOFC; direct and indirect hybrids may also be referred to as pressurized and atmospheric hybrids respectively.

Abbreviations: ER, expansion ratio; PR, pressure ratio; SOFC, solid oxide fuel cell; SOFC-GT, solid oxide fuel cell gas turbine; TIT, turbine inlet temperature; XTP, the inlet and outlet parameters of mass flow ($kg\,s^{-1}$), temperature (K), and pressure (atm).

* Corresponding author. Tel.: +1 907 978-2052; fax: +1 907 474-5475.
E-mail address: Winston.Burbank@gmail.com (W. Burbank Jr.).

[1] Credit also belongs to Dr. Wolf of Brayton Energy, LLC, Hampton, New Hampshire for his role as an advisor.

0378-7753/$ – see front matter © 2009 Elsevier B.V. All rights reserved.
doi:10.1016/j.jpowsour.2009.04.004

Nomenclature

el	moles of an element with a gas species (mol)
El	total moles of an element within a gas mixture (mol)
ER	turbine expansion ratio
h	specific enthalpy (kJ kg^{-1})
H	total gas mixture enthalpy (kJ s^{-1})
k	interpolated value for turbine speed lines
MS	normalized mach speed
ploss	pressure loss across a module (%)
P	total gas mixture pressure (atm)
Q	heat flux (kJ s^{-1})
rec	SOFC anode exhaust recycle (%)
SS	shaft speed
SX	shaft speed multiplier
T	gas mixture temperature (K)
W	work flux (kJ s^{-1})
x	species mass flow (kg s^{-1})
X	total gas mixture mass flow (kg s^{-1})

Greek symbol

ϕ	corrected mass flow (kg s^{-1})

Subscripts

C	compressor
cold	cold side of the heat exchanger
hot	hot side to the heat exchanger
i	index of single gas species
in	flow entering module
out	flow exiting module
ref	reference state of 25 °C at 1 atm
T	turbine

The concept of a fuel cell turbine hybrid has been discussed for many years (patented by Ztek in 1996 [2–4]). However, to date only a few SOFC-GT hybrid systems have been built and operated in demonstrations, the most publicized being the Siemens 220 kW pressurized SOFC, operated at the University of California at Irvine (Southern California Edison). While the 220 kW system operated successfully for 3250 h, instabilities plagued the system when operated outside its narrow design envelope [5]. Siemens has not proposed building another pressurized hybrid, and none are currently scheduled. Their website indicates since 2002 only two fuel cells have been scheduled for deployment, in 2005 and 2006, however, both currently have unreported hours of operation [6].

Rolls Royce Fuel Cells has worked on developing a direct/pressurized SOFC-GT hybrid [7]. The Rolls Royce configuration is unique in its use of custom designed ejectors to recycle both anode and cathode exit gases without the need for high temperature blowers/fans to accomplish anode recycling. In an effort to satisfy the airflow and cooling needs of the pressurized SOFC (without the need for additional bypasses, controls, or valves) Rolls Royce has been in the process of developing/modeling a custom two-stage/two spool turbocharger [8]. However, due to the large pressure drop across the ejectors and fuel cell, the turbomachinery will likely not contribute a significant amount of electrical power as compared to that supplied by the SOFC.

FuelCell Energy demonstrated an indirect 200 kW molten carbonate fuel cell hybrid, however published performance data could not be located.

Development of SOFC-GT hybrids has been hindered by the difficulty of finding off-the-shelf equipment that satisfies the air delivery/thermal profile requirements of an SOFC and the cost and complexity of developing custom turbomachinery [9]. Systems built to date have used bleed values, cathode bypasses, and variable speed turbines are used to correct the discrepancy of airflow to thermal management. However, these methods carry the penalties of lower system efficiency and more complex control strategies [9].

Researchers at the National Fuel Cell Research Center (NFCRC), the National Energy Technology Laboratory (NETL), and the Thermochemical Power Group (TPG) have published modeling results of SOFC-GT hybrids systems through individual and collaborative efforts. Direct SOFC-GT hybrid models and laboratory tests have been published [9–17]. Both TPG and NETL have test rigs able to model "hardware-in-the-loop" systems, thus validating computational models [11,16,18]. NFCRC with collaborators have published several transient studies as well as control strategies for indirect SOFC-GT hybrids and molten carbonate fuel cells (MCFC) hybrids [19–22]. Several studies have shown large turndown in both direct and indirect hybrids, but decreasing the fuel cell stack temperature to achieve turndown has been required [19,22].

This study is a steady-state model of a pressurized SOFC-GT hybrid, where the turbomachinery supplies the necessary airflow to the SOFC at increased pressure and Nernst efficiency, and, in turn, the exhausted heat from the SOFC powers the turbomachinery. The proposed system is unique in the use of a variable-geometry inlet vane turbine, which allows the system airflow to be controlled, thus maintaining the thermal needs of the SOFC. This allows a wide turndown ratio with high efficiency, while maintaining a constant SOFC stack exit temperature of 1000 °C, without the need for bleeds or bypasses. The decision to maintain the stack exit temperature at 1000 °C has been made with the hope that future transient analysis will find minimal thermal transients/gradients within the SOFC, allowing the system to respond to quickly and safely to electrical transients. The proposed system is also unique in that the turbomachinery contributes significantly more power than previous systems, actually delivering more power than the SOFC at design point [8–11,17,19–31]. Thus the total cost per kilowatt is lowered for the system. During turndown the turbomachinery continues to supply the airflow/cooling needs of the SOFC, but contributes proportionally less power, taking advantage of the high efficiency of fuel cells at low power. As a result, the proposed system's efficiency increases during turndown, while the ΔT across the SOFC stack remains below 200 °C.

Due to the wide turndown of the proposed hybrid, base loads can be supplied while also meeting the higher valued peak power demands. The proposed system may be found economical in distributed generation applications of stand-alone use, peak shaving, rural and remote generation, and combined heat and power (CHP) when fuel resources are available. However, due to the proposed systems higher capital and fuel costs, compared to that of coal, nuclear, hydro, and wind power plants, the SOFC-GT hybrid will likely not be economic for standby or base load operation when grid power is available [32].

2. System configuration

The proposed turbomachinery for use in the proposed system could be considered a micro-turbine cousin of the Northrop Grumman/Rolls-Royce WR-21 engine, soon to be deployed by the British Royal Navy [33-35]. A schematic of the proposed system is shown in Fig. 1, where the SOFC is the primary addition to the WR-21 configuration placed between the heat exchanger and the burner. The goal of this study is to allow a large turndown while maintaining the SOFC stack exit temperature at 1000 °C, using constant fuel utilization of 85%, and without the need for cathode

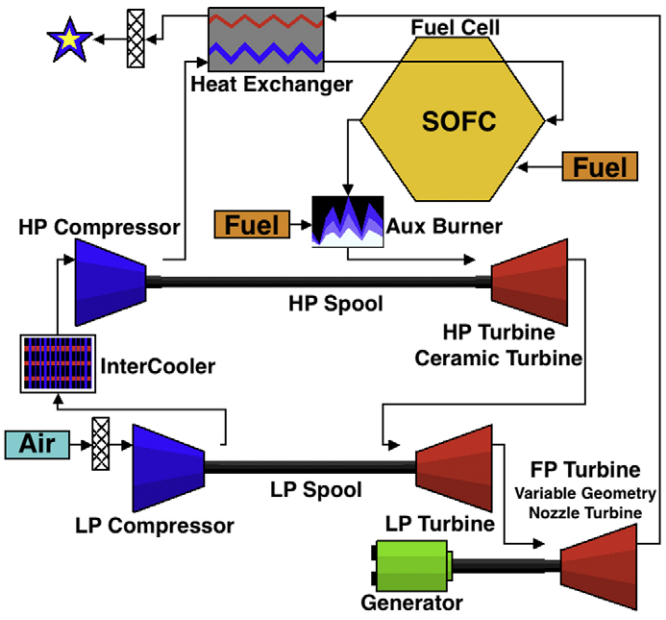

Fig. 1. Schematic of SOFC-GT hybrid engine.

bypasses and/or bleeds. This is accomplished using individual fuel controllers for both the SOFC and the auxiliary burner and incorporating two novel, yet commercially viable components [36]. First, a ceramic turbine is placed on the high-pressure spool, allowing higher turbine inlet temperatures (TIT) (controlled by the auxiliary burner). Secondly, a variable-geometry inlet nozzle turbine placed after the low-pressure spool allows an additional degree of freedom in system optimization and control. This variable-geometry nozzle turbine is referred to as the "free" turbine, as it is not attached to a compressor. The system is fueled by pure methane assuming a lower heating value of $-50026\,\mathrm{kJ\,kg^{-1}}$.

The non-hybrid turbine configuration (same schematic as Fig. 1 minus the SOFC) has been proposed as a diesel bus engine replacement, and as such, is designed so that the physical volume is quite compact [36]. The compact design minimizes the plenum volume, which is expected to decrease both transient instabilities and the amount of expensive high temperature piping. Single shaft spools are chosen to minimize vibration concerns, and radial compressors and turbines are chosen so that inexpensive off-the-shelf turbocharger-like compressors and turbines can be utilized.

The system in this study (Fig. 1) uses two separate single shaft turbochargers (each similar to what can be found today on many diesel engines). These turbochargers are compact, simple, and relatively inexpensive when mass-produced. The inlet ambient air passes through a filter into the low-pressure compressor, designed for a pressure ratio (PR) of 3. An intercooler reduces the air temperature entering the second, high-pressure compressor, designed for a PR of 5. The air is preheated by the heat exchanger and enters the SOFC module. Fuel flow into the SOFC is controlled such that the stack exit temperature remains at the prescribed level of 1000 °C. The SOFC exhaust enters the auxiliary burner with its own fuel controller optionally adding additional fuel, allowing independent control of the high-pressure turbine inlet temperature (TIT). The independent control of the high-pressure TIT allows for control separation of the turbomachinery from the SOFC. The combustion products then are expanded through the high-pressure and low-pressure turbines, supplying the torque requirements to their respective/attached compressors (accounting for isentropic inefficiencies and mechanical bearing losses). The exhaust then passes through the free turbine (the variable-geometry nozzle turbine) before flowing through the heat exchanger and exiting the system.

The SOFC is modeled as shown in Fig. 2, based on a Siemens Westinghouse tubular yttria-stabilized zirconia SOFC. The inlet air is preheated by an internal heat exchanger before entering the cathode. The inlet fuel (methane) mixes with a slipstream of anode off-gases to initiate steam reformation. The anode recycle is fixed at 65% throughout this study. Nernst voltage losses are calculated from average hydrogen and oxygen concentrations, stack exit temperature, pressure, and current density as given in the Fuel Cell Handbook 7th edition [37]. The anode and cathode off-gases exit at the same temperatures and are combusted before passing through the heat exchanger and exiting the SOFC.

3. Modeling

Due to the complexity and expense of building and operating fuel cell systems, much effort has been dedicated toward computational modeling of such systems. Modeling fuel cell systems allows for exploration and development of controls that would otherwise be both expensive and difficult to achieve in a physical system. When studying a novel engine configuration, steady-state analysis at multiple states can be used to predict the efficiency and performance of the proposed system. Steady-state analysis predicts dangerous operating zones, such as excessively high temperatures, large thermal gradients, and compressor surge. Transient analysis will be needed to understand how to control the engine from one steady-state operation mode to another, and is beyond the scope of the work reported here.

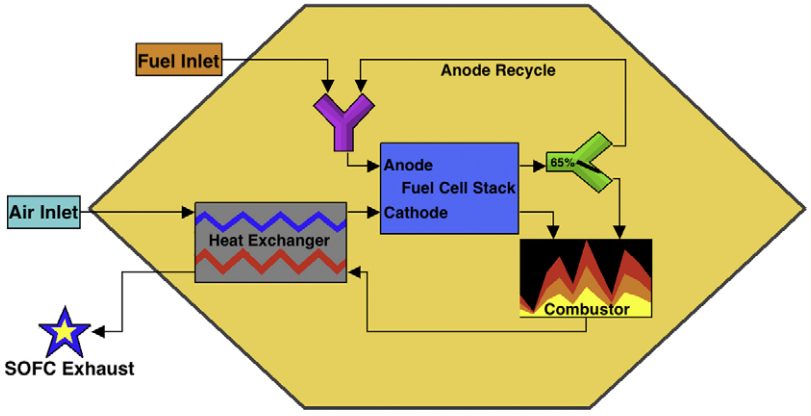

Fig. 2. Internal schematic of the modeled SOFC.

3.1. Model methodology

The steady-state model used in this work consists of lumped parameter components that express a balance between inlet and outlet flows of mass and energy (see Eqs. (1)–(3)). Each component of the system is modeled by calculating the exiting gaseous mass flow, temperature and pressure (XTP) for use in the next component. Pressure drops experienced across components of the system are an assumed fixed percentile loss, described by Eq. (5). Thermodynamic properties and calculations of individual gas species and/or mixtures are accomplished through the use of Cantera, a thermodynamic toolkit developed at CalTec [38]. Cantera uses NASA polynomials of heat capacity to calculate enthalpies, entropies, and Gibbs energies. Thirteen gaseous species are considered, although more can readily be added. These are CO, CO_2, H_2, H_2O, N_2, O_2, Ar, CH_4, C_2H_6, C_3H_8, C, NO, and NO_2. In the case of electro-chemistry, reformation, or combustion, conservation of mass is verified through a calculation of conservation of elements (Eq. (4)) verifying that an equal number of carbon atoms exit as had entered.

Enthalpy:

$$H = \sum x_i h_i \tag{1}$$

Conservation of energy:

$$H_{\text{out}} = H_{\text{in}} + Q - W \tag{2}$$

Conservation of mass:

$$X_{\text{in}} = X_{\text{out}} = \sum x_i \tag{3}$$

Conservation of elements:

$$El_{\text{in}} = El_{\text{out}} = \sum el_i \tag{4}$$

Pressure loss:

$$P_{\text{out}} = P_{\text{in}}(1 - \text{ploss}) \tag{5}$$

Compressor and turbine: Turbomachinery is modeled using experimental maps for each compressor and turbine component, providing pressure and flow data at various tip mach speeds. The compressor module calculates the normalized inlet mass flow, ϕ_C (Eq. (6)), and the normalized mach speed (Eq. (7)) from the given inlet XTP (mass flow, temperature, pressure) and shaft speed parameters. Knowing the inlet ϕ_C and mach speed, the pressure ratio (PR) and isentropic efficiency are calculated from smoothly interpolated parameterized polynomials fitted to the experimental maps. Output temperature and the required work for compression are found by first assuming isentropic compression of the calculated PR, and adding the efficiency penalty to the change in enthalpy.

Compressor corrected mass flow:

$$\phi_C = \frac{X_{\text{in}}\sqrt{T_{\text{in}}/T_{\text{ref}}}}{(P_{\text{in}}/P_{\text{ref}})} \tag{6}$$

Normalized mach speed:

$$MS = \frac{SS \times SX}{\sqrt{T_{\text{in}}}} \tag{7}$$

The normalized turbine maps have been fitted using Eq. (9), where intermediate speed lines are calculated by linearly interpolating k. Efficiency of the turbine is determined from a U/Co approximation [39–41]. Each compressor/turbine spool is directly linked via a rotating shaft with mechanical bearing losses equal to a percentage of the transferred power from the turbine. Within the turbine module, normalized mass flow, φ, is found from the inlet XTP parameters (Eq. (8)). The required expansion ratio (ER) is iteratively solved to meet the power requirements of the attached compressor, accounting for bearing losses and turbine efficiency. Outlet temperature is solved similarly to the compressor, assuming isentropic expansion and adding the inefficiency penalty. Knowing ϕ_T and ER, the mach speed of the turbine and the shaft speed of the spool are calculated. The system-wide solver minimizes discrepancies between the turbine shaft speed and the assumed input compressor shaft speed as is discussed in Section 3.2.

Turbine corrected mass flow:

$$\phi_T = \frac{X_{\text{in}}\sqrt{T_{\text{in}}}}{P_{\text{in}}} \tag{8}$$

Predicted turbine corrected mass flow:

$$\phi_T = 1 - e^{(-k(ER-1))} \tag{9}$$

Intercooler: The intercooler is placed between compressor stages and is simply modeled as decreasing the gas stream temperature to 3.9 °C above that of the ambient air temperature [36]. It is assumed that a blower, moving ambient air, will be able to meet the required heat exchanger effectiveness. The parasitic load of the blower is assumed to be a constant 6.0 kW.

Heat exchanger: The primary heat exchanger/recuperator, as well as the SOFC's internal heat exchanger, are modeled using the number of transfer units (NTU) method to solve the outlet temperatures, given a prescribed effectiveness (Eq. (10)). Outlet pressures on the primary heat exchanger are found from prescribed pressure drops of 2.0% and 2.8% on the cold and hot sides, respectively.

Heat exchanger NTU method:

$$H_{\text{hot out}} - H_{\text{hot in}} = \Delta H = H_{\text{cold out}} - H_{\text{cold in}} \tag{10}$$

Combustor/burner: The species output of the combustor module is found using Canteras' equilibrium function, which solves for the Gibbs energy minimization dependant upon outlet temperature, pressure, and the considered species. A prescribed heating value loss of 2.8% is assumed in the auxiliary burner.

Variable-geometry nozzle turbine: The free turbine, named for not being connected to a compressor, is modeled similarly to the above turbine with two differences due to the variable nozzles. First, the turbine map is stretched along the corrected mass flow (φ) axis according to the percentage of the vanes' opening. Secondly, an efficiency decrement is added to the U/Co departure [42]. The outlet pressure is set at what is required for exhausting the gas, and the mach speed is found such that the turbine may operate at highest efficiency. The work produced by the turbine is transferred to a variable speed generator, where an 8% power loss from turbine to deliverable AC is calculated, due to mechanical and electrical losses.

SOFC: The fuel cell module (set up to model a Siemens Westinghouse yttria-stabilized zirconia (YSZ) SOFC) is modeled as depicted in Fig. 2. Characteristics include a 65% anode recycle, allowing prereforming of the incoming fuel, an air pre-heater and an off-gas combustor. It is assumed that the anode and cathode streams exit at equal temperatures. Cell voltage/Nernst losses are calculated considering stack exit temperature, exit pressure, average hydrogen and oxygen concentrations, and average current density using equations and data provided on pages 7–20 through 7–31 of the Fuel Cell Handbook 7th edition [37]. The SOFC module iteratively solves for the appropriate fuel flow into the anode to meet the prescribed stack exit temperature, given the fixed fuel utilization, and

constant heat exchanger effectiveness. It is assumed that the anode recycle composition is equal to that of the anode exit. The normalized mass flow of the recycle stream, at steady state, is found by multiplying the anode exit by Eq. (11).

The recycle stream mixes with the fuel inlet stream to initiate reformation. (This model does not include any energy required for the ejector or blower within the recycle stream.) An average gas concentration across the fuel cell stack is required to calculate the Nernst voltage drop on the anode side due to concentrations of hydrogen and steam. The average is calculated from the compositions of the inlet reformed fuel with the anode recycle and the anode exit.

The reformation of the inlet fuel with the anode recycled offgas is done by modeling a steam reforming reaction followed by a water gas shift reaction that produces only H_2, CO_2, CO, H_2O, O_2, and CH_4. The anode outlet composition is calculated using a Gibbs minimization, dependant upon outlet temperature and pressure. The voltage drop due to the use of methane as opposed to pure hydrogen, at a fuel utilization of 85%, is found to be −24.1 mV, consistent with numbers used by industry.

The anode and cathode streams are then adiabatically combusted as described above in the combustor module (Gibbs minimization). The products then exit the SOFC module through a heat exchanger preheating the incoming air. The fuel flow required to meet the desired stack exit temperature is reached using the Matlab® fsolve function (a Newtonian solver). Lastly the XTP parameters of the combustion products exiting the SOFC's heat exchanger are passed out of the module, along with the net power produced assuming a 10% loss due to the DC to AC electric conversion.

Mass flow of recycle stream:

$$X_{\text{rec}} = \frac{\text{rec}}{(1 - \text{rec})} \tag{11}$$

Additional assumptions:

- The energy parasitic of fuel compression is not considered in this study, due to the large variability in how methane can be delivered.
- The effectiveness of both the stand-alone heat exchanger and the internal heat exchanger within the SOFC is assumed to be constant throughout the study.

3.2. System-wide solver/convergence

The system as depicted in Fig. 1 is solved using Matlab's® multivariable solver fsolve, which computes a discrete Jacobian Matrix, and iteratively varies all system variables in search of minimizing the returned vector. The returned vector consists of the difference between the guessed values and the calculated desired values of the system. The system in this study requires four variables to be solved simultaneously. These variables are: the low-pressure spool shaft speed, the high-pressure spool shaft speed, the exit temperature from the heat exchanger on the cold/pressurized side, and lastly, the inlet air mass flow. The low-pressure and high-pressure compressor shaft speeds are compared to the desired operating speed of their corresponding turbine, having met the compressor power. Likewise, the system assumes an outlet temperature on the heat exchanger cold side. This value is then compared with the calculated value once the hot side inputs have been calculated. Lastly, the ambient air entering the system is assumed and compared to what value is required by the free-pressure turbine (the variable-geometry nozzle turbine) to be at its peak efficiency. Using good initial values and many computational iterations, the above four variables are found such that the errors/differences approach zero (less than 10^{-4} difference).

3.3. Design point

The design point for the proposed system is set using multiple parameters. The primary parameters are the designed pressure ratio and surge margin of each compressor, the primary heat exchanger's effectiveness, the design point fuel cell voltage, the fuel cell stack exit temperature, the fuel cell module exit temperature (after the internal heat exchanger), the fuel cell fuel utilization and anode recycle, the high-pressure turbine inlet temperature (TIT), and finally, the system airflow. Values of pressure loss are assigned to most components, and are considered constants throughout the study. The model uses specialized code to solve the system and calculates values that are then used for all off-design analysis. For each compressor a mach speed multiplier, pressure ratio (PR) multiplier, and a normalized mass flow multiplier are reported. These multipliers are used for *stretching* the compressor map and are in the range of ±7%. Each turbine reports a multiplier for normalized mass flow, shaft speed, and *U* (the tip speed). The SOFC reports the cell area required to satisfy the current density needed to meet the desired voltage at design point, and reports the internal heat exchanger effectiveness, which meets both the prescribed stack exit temperature and module exit temperature.

For further clarification, each compressor/turbine is *stretched* to meet the design point conditions, however once the *stretching* parameters are determined they remain fixed for all off-design modeling. This also includes the SOFC where the cell area and internal heat exchanger effectiveness are determined for the design point. However, the cell area and heat exchanger effectiveness then remain fixed and constant for all off-design modeling. The design point conditions are displayed in Table 1.

4. Results

A safe and optimized turndown strategy has been found for the proposed engine after simulating more than 800 conditions of varied high-pressure TIT and variable-geometry nozzle settings. Performance graphs of the proposed engine are presented below in Figs. 3–12 . The black bold line with diamonds on Fig. 5 represents the highest efficiency at varied power levels while respecting safe operating constraints. This line represents what is herein referred to as the turndown line. Safe operation constraints include: a surge margin greater than 5% on both the low-pressure and high-pressure

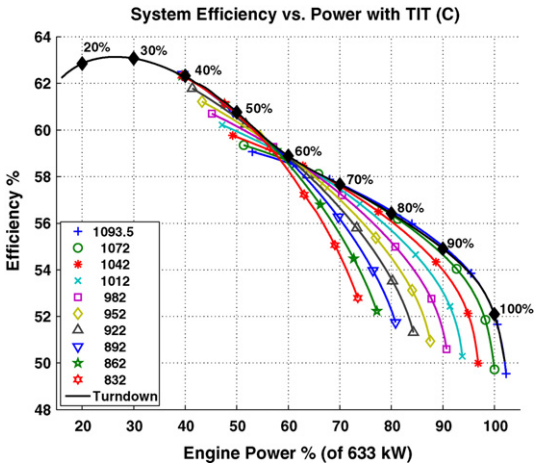

Fig. 3. SOFC-GT system electrical efficiency vs. rated system power. 100% of rated system power corresponds to 640.74 kW of produced power.

Table 1
Design point configuration data.

Design point			
TIT		1093.35 °C	
Inlet air flow		1.172 kg s^{-1}	
System work		646.704 kW	
System efficiency		53.19%	
Turbomachinery	PR or ER	Efficiency (%)	Inlet temperature (°C)
LP compressor	3	73.79	15.00
HP compressor	5	79.75	18.90
HP turbine	2.02	83	1093.35
LP turbine	1.68	85	922.38
FP turbine	3.78	85	804.86
Intercooler			
ΔT approach		Pressure loss	
3.9 °C		2.0%	
Heat exchanger			
Effectiveness	Cold side inlet temperature	Hot side inlet temperature	Cold side pressure loss / Hot side pressure loss
90%	230.24 °C	550.28 °C	2.0% / 2.8%
SOFC			
Fuel utilization			85%
Anode recycle			65%
Voltage			0.5 V
Average current density			720.772 mA cm^{-2}
Stack exit temperature			1000 °C
Modular exit temperature			850 °C
Heat exchanger effectiveness			47.48%
Cell area			941996 cm^2
Anode pressure loss			5%
Cathode pressure loss			5%
Combustor pressure loss			0%
Heat exchanger pressure loss			0%
Auxiliary burner			
Pressure loss		Combustion efficiency	
2.80%		97.20%	
Mechanical bearing losses			
Low-pressure spool	High-pressure spool	Free-pressure spool	
2%	2%	8%	
Inlet filter pressure loss		0.50%	
Outlet filter pressure loss		0.50%	

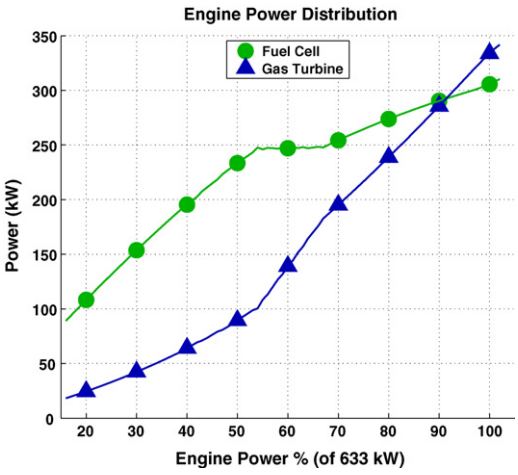

Fig. 4. Power sharing characteristics vs. rated power. *Note*: 6 kW intercooler blower parasitic is not accounted for in this figure.

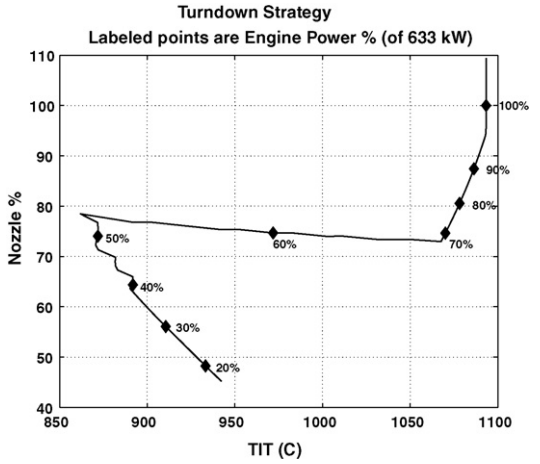

Fig. 5. The 5:1 turndown strategy of the SOFC-GT hybrid. Labeled percentages indicate the engines rated power. The large TIT reduction experienced between 70% and 55% of the engines rated power may lead to difficult thermal transients.

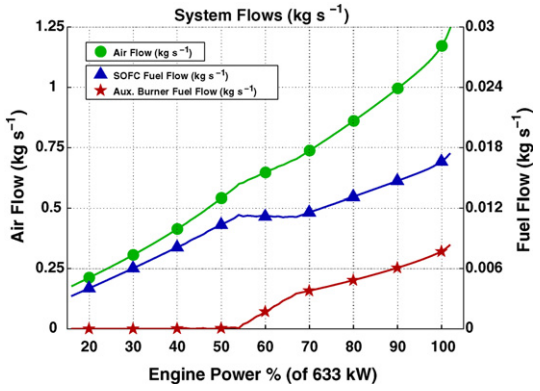

Fig. 6. System airflow is shown as the top line with circles (left axis). Fuel flow to the SOFC is shown with triangles, while the aux. burner is indicated with stars (right axis).

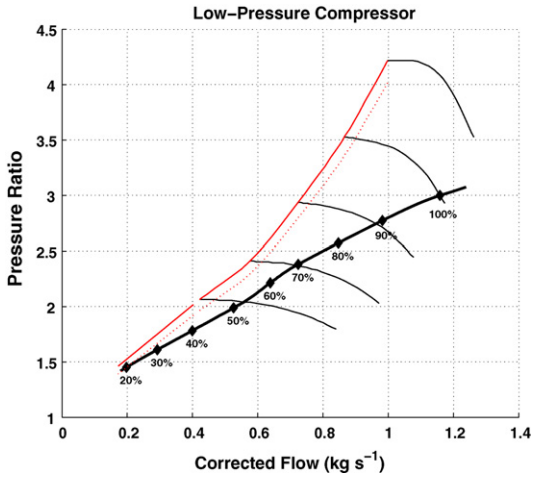

Fig. 7. Performance of the low-pressure compressor during turndown. Labeled percentages are the engines rated power.

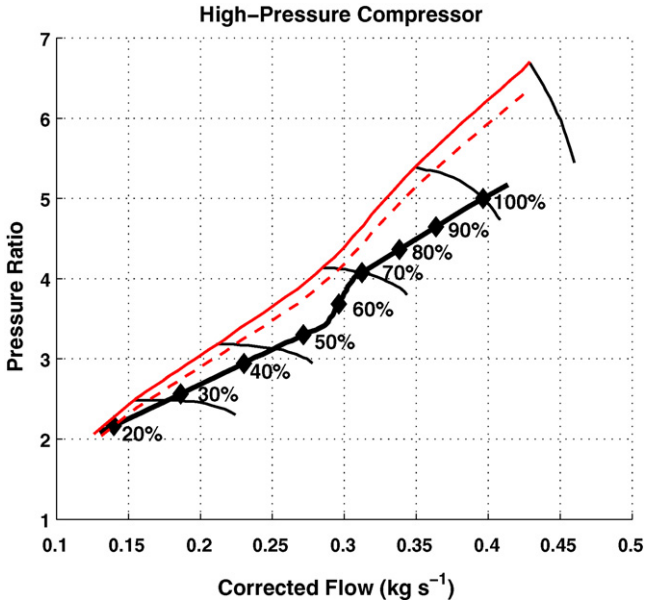

Fig. 8. High-pressure compressor performance during turndown.

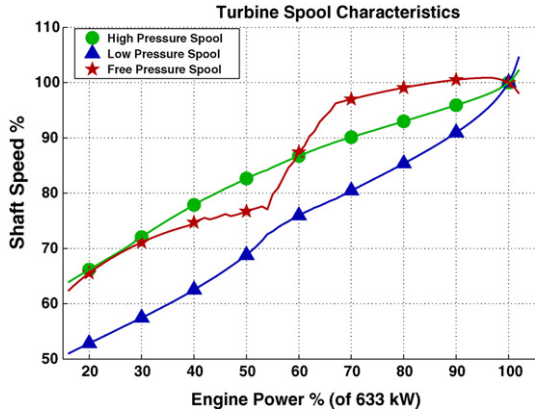

Fig. 9. The percentage of rated shaft speed for each turbine during turndown.

compressors, TIT not exceeding 1093.3 °C (2000 °F) on the high-pressure ceramic turbine, and TIT not exceeding 927 °C (1700 °F) on the low-pressure turbine [36]. Diamonds are plotted on all plots in order that a correlation can be made between figures based upon the turndown percentage.

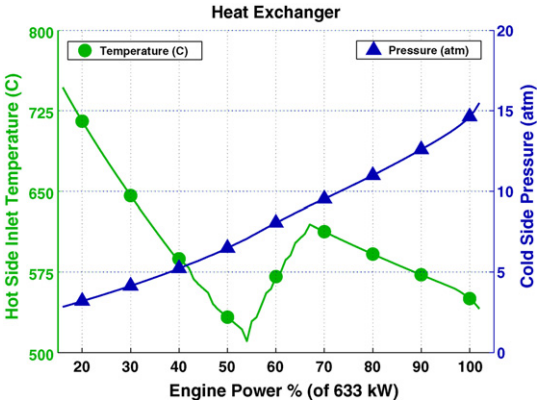

Fig. 10. The heat exchanger extreme profiles of temperature and pressure. Temperature is from the exhaust (unpressurized and hot) side and pressure is taken from the pressurized (air inlet) side.

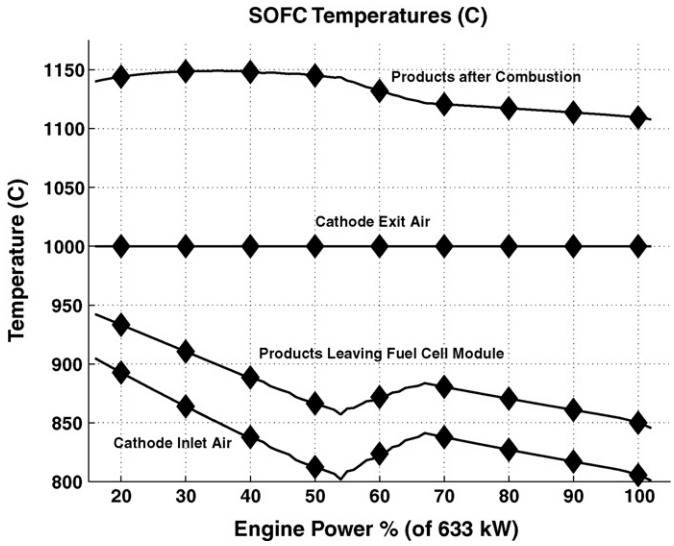

Fig. 11. Temperature profile within the SOFC.

Fig. 3 displays the system efficiency vs. rated engine power accounting for the 6 kW intercooler blower parasitic. While the turndown line visually appears to hug the peak TIT line, the author can view, when zoomed in, the turndown line slowly decreasing, as is shown in Fig. 5, between the range of 95% and 70%. From the design point of 633.48 kW to a turndown of 126.7 kW the efficiency increases from 52.1% to 62.85%. This is due to the unique characteristic that at design point the power produced is evenly split between the free-pressure turbine/generator and the SOFC. As the airflow is reduced, the turbine contributes relatively less power, thus allowing the highly efficient SOFC to raise the system efficiency.

Fig. 4 shows the power contributed by the SOFC and the variable-geometry nozzle turbine. At design point the turbine produces slightly more power than the SOFC. This shared distribution of power at design point is expected to lower system capital costs as turbomachinery typically costs between \$300 kW^{-1} and \$500 kW^{-1}, while SOFC prices are estimated at \$1500 kW^{-1} and above [23,43]. Thus a significant portion of the rated power will come from the less expensive turbomachinery, resulting in a lower cost per kW of the system.

Fig. 5 shows the control strategy required for the engine to follow the peak efficiency turndown, where the labeled black diamonds represent the engine's percent of rated power. Below 50% turndown, supplemental heating is not required and fuel flow into the auxiliary burner is stopped as seen in Fig. 6. The high-pressure TIT

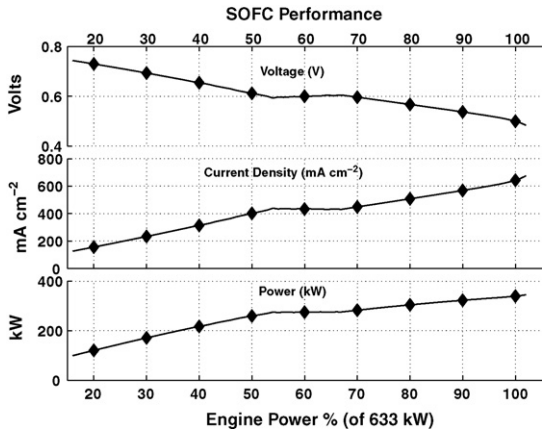

Fig. 12. SOFC performance profiles of stack voltage, current density and power.

is generated by the SOFC exhaust. Please note the TIT below 50% turndown is not the 1000 °C from the stack exit, but rather the SOFC module exhaust after preheating its own inlet air. Turndown continues to 20% by reducing the variable-geometry turbine nozzle settings.

Figs. 7–9 display the operating characteristics from the low-pressure compressor, the high-pressure compressor, and the turbine spool speeds, respectively. Notice on the compressor plots, Figs. 7 and 8, that an unusually large surge margin is chosen as the design point in order to maintain surge margin during turndown, which also carries an efficiency decrement. It is also important to note that compressor maps were chosen with wide and shallow surge lines for this same reason. Figs. 7 and 8 as well as the omitted turbine performance maps closely resemble those published by Brayton Energy for the non-hybrid version of this engine [36]. At 20% turndown a surge margin of 5% is held by both compressors, however if turndown continues to 16% the surge margin approaches zero, thus a 5:1 turndown is deemed safe. Fig. 9 displays the percent deviation from the design point shaft speed for all turbine spools during turndown. The choice of variable speed generator will need to consider the 65% reduction in shaft speed experienced by the free-pressure turbine.

Fig. 10 shows the hot (exhaust) side temperature and the cold (inlet air) side pressure of the heat exchanger. These two parameters represent the extremes experienced by the heat exchanger. At turndown levels below 30% the temperature increases into ranges where high temperature materials may be required. Despite this increased temperature in this range the pressure differential is less than 4 atm.

Fig. 11 shows five different temperatures within the SOFC module throughout the turndown: the cathode air inlet (after preheat), the cathode exit, the post combustion of the anode and cathode streams, and lastly, the discharge from the SOFC module (after preheating the inlet air), as is depicted in Fig. 2. The proposed engine allows the cathode exit to maintain its 1000 °C criteria throughout a 5:1 turndown, and limits the change in temperature across the cathode (from inlet to its outlet) to less than 200 °C.

Fig. 12 displays the SOFC operating voltage, average current density, and DC power output. Note both the anode and cathode of the SOFC are pressurized similarly to that experienced by the heat exchanger's cold side as shown in Fig. 10, thus the increased pressure allows higher current densities and performance benefits within the SOFC. A fuel compressor is needed to supply methane at pressures matching that of the supplied air, however this study does not model the fuel compressor for either the SOFC or auxiliary burner. Inclusion of a fuel compressor is expected to add a significant parasitic to the system.

5. Discussion

The results from the steady state analysis are promising: the proposed SOFC-GT hybrid shows stable operation over a wide turndown ratio of 5:1 with remarkably high efficiencies that increase during turndown. This configuration with the ability to operate at low power levels may make startup and shutdown less stressing to the system components. The simple turbocharger-like (single shaft) compressor/turbines used for the low and high-pressure spools are expected to minimize shaft dynamics and instabilities [36]. Short plumbing interconnects are expected to minimize transient instabilities and minimize the use of high temperature metals.

Additional modeling work is necessary: transient analysis is particularly needed between the range of 70–55% turndown, due to the rapid temperature gradient experienced by the hot components as shown in Figs. 5 and 10. The largest thermal difference is experienced by the high-pressure turbine where between 70% and 55% turndown the TIT deceases 208 °C as seen in Fig. 5. However, due to the ability to separately control TIT (with the auxiliary burner) and system air flow (with the variable-geometry turbine nozzles) there is hope the proposed system may respond to electrical transients using the turbo machinery for quick changes while simultaneously maintaining slow thermal management/transients of the SOFC.

In the future, testing of the proposed hybrid may be possible through a simulated (*hardware-in-the-loop*) fuel cell, as a non-hybrid configuration of the turbine may become available as an alternative to a diesel bus engine [36]. The system capital costs will be significantly lower than that of a stand-alone fuel cell due to the nearly equal sharing of rated power between the expensive SOFC and the lower cost turbomachinery. Due to the unique characteristic of increased efficiency throughout turndown, the decision to purchase additional capacity either for future growth or for operating the engine at less than rated power for increased efficiencies could prove economical.

As mentioned in the Brayton Energy paper [36], incorporating variable inlet-guide vanes on the low-pressure compressor could increase the surge margin at low turndown and increase the compressor efficiency at design point. Increased turndown and/or startup procedures may be found if the SOFC stack temperature is allowed to decrease below the fixed 1000 °C.

6. Conclusions

While SOFC-GT hybrids show great electrical efficiencies at design point, previous designs have narrow operating ranges. The proposed SOFC-GT hybrid shows the possibility of meeting a turndown ratio of 5:1 while retaining remarkably high efficiencies. This is done while maintaining the SOFC stack exit temperature at 1000 °C, limiting the ΔT across the stack to less than 200 °C, and keeping a constant fuel utilization of 85%. The proposed engine warrants additional research and should be considered a candidate for future pressurized SOFC-GT hybrid demonstrations.

Acknowledgements

Thanks to the Department of Defense for sponsoring the work presented above through contract number W9132T-04-2-007. The content of this report does not necessarily represent the position or policy of the government and no official endorsement should be inferred.

References

[1] J. Larminie, A. Dicks, Fuel Cell Systems Explained, John Wiley & Sons Ltd., 2003.
[2] M.S. Hsu, Pressurized, Integrated Electrochemical Converter Energy System, Ztek Corporation, 1999.
[3] M.S. Hsu, E.D. Hoag, Electrochemical Converter Having Internal Thermal Integration, U.S.P. Office, Editor. Ztek Corporation, Waltham, Mass. 1996, p. 12.
[4] M.S. Hsu, E.D. Hoag, Ultra-High Efficiency Turbine and Fuel Cell Combination, U.S.P. Office, Editor. Ztek Corporation, Waltham, Mass. 1997, p. 14.
[5] K.P. Litzinger, ASME ICEPAG, Irvine, CA, 2005.
[6] Siemens, Siemens Power Generation - SOFC Solutions Provider, 2008 [cited 2008 5/29/08]. Available from: http://www.powergeneration.siemens.com/products-solutions-services/products-packages/fuel-cells/demonstrations/demonstrations-summary/.
[7] D.G.D. Agnew, ICEPAG, Irvine, CA, 2004.
[8] S.G. Berenyi, ICEPAG, Irvine, CA, 2004.
[9] A. Traverso, et al., Journal of Fuel Cell Science and Technology 4 (November) (2007) 11.
[10] P. Costamagna, L. Magistri, A.F. Massardo, Journal of Power Sources 96 (2) (2001) 352–368.
[11] M.L. Ferrari, et al., Journal of Engineering for Gas Turbines and Power 129 (October) (2007) 8.
[12] M.L. Ferrari, et al., Journal of Power Sources 149 (2005) 22–32.
[13] O. Grillo, L. Magistri, A.F. Massardo, Journal of Power Sources 115 (2003) 252–267.
[14] T. Kaneko, J. Brouwer, G.S. Samuelsen, Journal of Power Sources 7773 (2006).

[15] L. Magistri, et al., Journal of Engineering for Gas Turbines and Power 129 (July) (2007) 6.
[16] M. Shelton, et al., ASME Turbo Expo, ASME, Reno, NV, 2005.
[17] D. Tucker, et al., ASME Turbo Expo, ASME, Reno, NV, 2005.
[18] M. Pascenti, et al., ASME Turbo Expo 2007, Montreal, Canada, 2007.
[19] F. Mueller, et al., Journal of Fuel Cell Science and Technology 4 (August) (2007) 10.
[20] R. Roberts, et al., Journal of Power Sources 161 (1) (2006) 484–491.
[21] R. Roberts, et al., Journal of Engineering for Gas Turbines and Power 128 (April) (2006) 8.
[22] R.A. Roberts, et al., ASME Turbo Expo, ASME, Reno, NV, 2005.
[23] F. Calise, et al., Energy 32 (4) (2007) 446–458.
[24] J. Christopher, J. Steffen, J.E. Freeh, L.M. Larosiliere, Turbo Expo, 2005, NASA, Reno, NV, 2005.
[25] T.S. Kim, S.H. Hwang, Energy 31 (2–3) (2006) 260–277.
[26] A. Traverso, A.F. Massardo, R. Scarpelli, Applied Thermal Engineering 26 (2006) 1935–1941.
[27] A. Traverso, R. Scarpellini, A. Massardo, Experimental Results, AMSE Turbo Expo, 2005, ASME, Reno, NV, 2005.
[28] S.E. Veyo, et al., Journal of Engineering for Gas Turbines and Power 124 (October) (2002) 5.
[29] J.S. Yang, J.L. Sohn, S.T. Ro, Journal of Power Sources 166 (1) (2007) 155–164.
[30] J.S. Yang, J.L. Sohn, S.T. Ro, Journal of Power Sources 175 (1) (2008) 296–302.
[31] X. Zhang, et al., Journal of Power Sources 163 (1) (2006) 523–531.
[32] M.C. Williams, J. Strakey, W. Sudoval, Journal of Power Sources 159 (2) (2006) 1241–1247.
[33] J. Janes, ASME International Gas Turbine and Aeroengine Congress & Exhibition, Birmingham, UK, 1996.
[34] C.C.R.E.R. Navy, Proceedings of the International Gas Turbine Congress, Tokyo, 2003.
[35] Rolls-Royce, WR-21 Fact Sheet, 2000.
[36] T.L. Wolf, J.B. Kesseli, J.S. Nash, ASME TurboExpo 2008, Berlin, Germany, 2008.
[37] EG&G Technical Services, I., Fuel Cell Handbook (Seventh Edition), DOE, Morgantown, West Virginia, 2004.
[38] D.G. Goodwin, Cantera C++ User's Guide, 2002.
[39] M.G. Kofsky, W.J. Nusbaum, Aerodynamic Evaluation of Two-Stage Axial-Flow Turbine Designed for Brayton-Cycle Space Power System, NASA, 1968.
[40] H.E. Rohlik, Radial-Inflow Turbines, NASA, 1972, pp. 31–57.
[41] E.M. Szanca, H.J. Schum, Experimental Determination of Aerodynamic Performance, NASA, 1972, pp. 103–139.
[42] P.L. Meitner, A.J. Glassman, Off-Design Performance Loss Model for Radial Turbines with Pivoting Variable-Area Stators, N.L.R. Center, Cleveland, 1980.
[43] S.C. Singhal, K. Kendall, High-Temperature Solid Oxide Fuel Cells: Fundamentals, Design and Applications, Elsevier, 2003.